International Journal of Computing and Digital Systems
ISSN (2210-142X)
Int. J. Com. Dig. Sys. 13, No. 1 (Apr-23)

http://dx.doi.org/10.12785/ijcds/130187

Combined CNN with STARGAN for Wheat Yellow Rust Disease Classification

Deepak Kumar[1] **and Vinay Kukreja**[1]

[1]*Chitkara University Institute of Engineering and Technology, Chitkara University, Punjab, India.*

Received 11 Jul. 2022, Revised 25 Apr. 2023, Accepted 28 Apr. 2023, Published 30 Apr. 2023

Abstract: Experienced evaluators takes a lot of time for the correct prediction of wheat yellow rust. For better prediction of wheat yellow rust disease in wheat plant, computer assisted techniques such as machine learning (ML), deep learning (DL), image processing and computer vision techniques are employed. While considering these aspects, an automatic classification system for wheat yellow rust using a hybrid approach of a generative adversarial network (GAN) and convolutional neural network (CNN) is proposed. Also, the proposed model helps to identify wheat yellow rust disease at different severity levels (very low, low, medium, high, and very high). For achieving objectives about proposed model, State of Art GAN (STARGAN) helps in data augmentation of wheat plant disease images. Finally, a wheat rust model based on convolutional networks was trained on generated data. A case study has also been accomplished on the generated data by deploying a CNN model for classification. Then a comparative analysis of the proposed methodology has been consummated by differentiating the performance metric with the fully convolutional network, deep CNN (DCNN) and random forest models. A Deep CNN is a CNN model with a huge number of hidden layers. Comparing the proposed approach with other models, the proposed approach achieves a greater classification accuracy of 95.6% at a medium severity level.

Keywords: Wheat, Agriculture, Crop, Convolutional Neural Networks, Generative Adversarial Networks, Precision, Productivity

1. Introduction

The agriculture industry is the primary source of livelihood for half of India's population [1]. Agriculture exports are one of the major contributors to the Indian economy. Since it has become imperative to ensure a degree of quality when it comes to crop production. Due to fungal and bacterial diseases, the production rate of wheat and rice crops is decreasing early [2]. Therefore, it has become an important step to maintain a balanced production rate as it affects the Indian economy.

Yellow rust is a fungal disease and it has a significant effect on wheat production worldwide [3]. To prevent fungal infection in diseases, the detection of wheat yellow is a prerequisite and then a proper amount of fungicides mixed with soil along with an adequate amount of spray on the plant is required. If this process is effectuated manually by experienced evaluators or microscopic techniques, it becomes tedious to correctly find the disease-driven plants in time. To control these issues, real-time rust detection is a vital step [4]. For real-time detection, computer vision techniques are popularly used for disease recognition. Spectroscopic imaging technique [5] plays a vital role in computer vision techniques. Also, computer vision techniques work on images [6] and these images can either be captured from a camera/scanner or unmanned aerial vehicles/hyperspectral sensors [7]. However, these captured image techniques are based on the task specified and involve expertise awareness in an optimal experimental condition. Crop diseases can easily be identified through collected images using computer vision techniques [8], which take less time than molecular equipment [9]. Input images are analyzed with feature extraction techniques such as principal component analysis (PCA) and morphological operations, including clustering with K means [10], [11]. After extraction of color, shape and texture features, the features are then classified either using Visual Geometry Groups (VGG) based on deep learning techniques with different hidden layers (VGG16, VGG19, VGG-CNN-S, and VGG-CNN-VDD16) [12] or Support vector machine (SVM) [13]. Therefore, machine learning techniques achieve low classification accuracy as compared to deep learning techniques for wheat rust disease identification [14], [15].

To improve classification accuracy, only two of the

E-mail address: Deepak.k@chitkara.edu.in, Vinay.kukreja@chitkara.edu.in

hybrid models have been developed (CNN-LSVM [16] and Differential amplification CNN (DACNN) [17] for wheat rust disease identification. After the classification of crop diseases [18], [19] different severity levels of diseases are identified at a large scale. Hence, to avoid human error in wheat rust disease identification, some of the authors [20], [21], [22] have developed a mobile-based application [11], [18] that identifies the wheat rust disease automatically [23]. To our best knowledge, few researchers have reduced above mentioned diagnostic challenges [24] for wheat crop diseases. Therefore, to prevent human errors, an intelligent system is required that can warn farmers if the disease affects any portion of the harvest.

A. *Major contribution of this paper*

Major contribution of this paper is described as:

- The present study proposes a novel approach for enhancing image processing and classification using STARGAN and CNN functions.
- The principal objective of this paper is to determine whether neural networks are effective in detecting wheat yellow rust disease in wheat plant low-quality images.
- Even with low-quality images, the proposed model was able to effectively classify the diseased leaves against those with wheat yellow rust disease.

B. *Organization of this paper*

The paper follows the following structure: Section 2 sketches the related work. A full explanation of the methods used for wheat yellow rust prediction is defined in Section 3. A discussion of the experimental results and the results of the experiments is presented in section 4. A comparison between the proposed approach and state-of-the-art techniques for wheat yellow rust disease classification is discussed in section 5. As a final note, section 6 discusses the conclusion and future work.

2. Related work

Many authors deployed deep learning and machine learning techniques for various wheat rust diseases identification. Moshou et.al [4] present and compare the self-organizing map (SOM) and NN classifier for the distinguishing of wheat yellow rust at the development stage. For data preprocessing, the authors used the quadratic discriminant technique. Mo [5] built a prediction model for wheat yellow rust disease during different seasons such as summer, autumn, and spring season in Pingliang area of china. The training of these three season factors is calculated through function traingdx and prediction values of these factors lie in a range of 01.-0.4 using Backpropagation NN. The result shows [6] that the NN has high prediction accuracy than PCA in wheat rust disease identification. Wang et. al [7] implements the Artificial neural network (ANN) technique for wheat rust disease identification. Also, the author compares the ANN with PCA. The authors [8] compared the Continuous wavelet analysis feature with the raw reflectance conventional feature technique for the wheat stripe rust disease recognition at development stage.

The authors [9], [10] compare the Multilayer perceptron NN with Radial basis function (RBF) NN for the recognition of yellow rust and Tan spot wheat diseases. Many mobile applications [11], [18] have been developed for the identification of wheat rust and spot diseases. Pryzant et.al [19] compared the CNN and Recurrent NN (RNN) deep learning models with histogram buckets being wheat rust diseases prediction. The images were taken from CIMMYT and wheat rust is identified in the Ethiopia area. During the prediction of wheat rust diseases, the CNN and RNN have a higher area under the curve (AUC) than histogram buckets.

Lu et.al [12] presents a deep multiple-instance framework which is the combination of two architectures namely VGG-FCN-VD16 and VGG-FCN-S for wheat rust disease diagnosis. The authors [13] identify the wheat-healthy plant and wheat disease plant through K-means clustering and PCA. The authors [14] proposed a flood filter image processing algorithm for wheat leaf rust detection. Using red edge-based stress index technique, the authors [20] identified wheat yellow rust at various severity levels. Thus, a leaf blotch wheat disease was identified at four different severity levels (Low, very low, high, and very high) through CNN and SVM. During identification, CNN and SVM features have been compared with Color histogram, Vegetation index features.

According to many authors [25], wheat diseases can be classified using CNN frameworks such as VGG-16, and VGG-19. For wheat rust, streak, and spot disease classification, the authors proposed a matrix-based CNN (MBCNN) approach [26] and compared it to Alexnet and VGG16 pretrained models.

But during experimentation, MBCNN achieved higher accuracy than Alexnet and VGG16. The categorization of wheat kernels [15] has been identified through the deep learning framework VGG16 and SVM. The authors [16] proposed a hybrid approach known as CNN-LSVM and compare their approach with CNN-Softmax and CNN-SVM for wheat yellow rust identification. The authors [21] compare Continuous wavelet analysis features with the raw reflectance conventional feature technique for the identification of wheat stripe rust disease. Deep convolutional neural network (DCNN) has a excessive increasing speed than other NN techniques in wheat disease identification [12], [27].

The Authors [22] compare the DCNN with Random

forest for head blight wheat diseases recognition. The authors [17] present a novel approach known as Differential amplification CNN and combines DACNN with Softmax, SVM and K-nearest neighbor for wheat disease classification. The researchers [24] used machine learning algorithms namely RF, SVM and NN for determining the wheat lodging. Also, the authors used unmanned aerial system camera images for wheat lodging. During wheat lodging, the NN achieves a high recognition rate as compared to SVM and RF algorithms.

Table 1 shows the summarized information about the related work.

After reviewing the different studies for wheat diseases classification, the gaps were identified which are described:

- Each of the researchers [27], [15], [17] used their own collected dataset for wheat disease prediction. In terms of wheat disease prediction, no public dataset is available.
- Many authors [20], [24] used the hyperspectral imaging system for wheat disease prediction. The cost of a hyperspectral imaging system is too high and a laborious process that decreases the dynamicity of the recognition model.
- Different image processing techniques [12], [27] have been used to augment the real-time dataset but there is no automated image translation approach for finding the augmented dataset reality.

3. Methods

A. Outline

This section describes the proposed methodology for wheat yellow rust disease identification with different severity levels. So, the comprehensive dataset description has been narrated over section B. After dataset gathering, the dataset has been augmented for training purposes in the CNN model. In section C, the augmented model is described in detail. In Section D, a deep neural network is enlarged into original training dataset for calculate the classification accuracy. As a result of the classification of wheat yellow rust disease, several severity levels have been established that indicate the severity of the disease which has been expressed in section E. An evaluation of the network's ability to predict disease class is based on the images used in the testing. The overview of the proposed methodology has been shown in figure 1.

The proposed algorithm for wheat yellow rust disease classification is as follows:

- Find the availability of the rust diseases dataset.
- Compute the image positions (P_x).
- $P_x(i) = \mathrm{Im}_{r^* j}$ (1)

where P_x(i) is the dimensions of an image in form of pixels

- $P_x(i)_{pp}$ is the preprocessed image with the corresponding labels {L(i)} where i=1, 2, 3,4 the main aim of STARGAN is to generate translation images through cross-entropy loss function:

$$P\left(y^{(i)} = C \mid P_x(i)_{pp} : w\right) \tag{2}$$

Where P is the probability of class n with a given preprocessed image $P_x(i)_{pp}$

$$\begin{aligned} &\mathrm{Im}_{(wc)}\, P_x(i)_{pp} = C_1 + C_2 \cdots - C_n + P_1 + P_2 \cdots P_n + \\ &Inc_1 + \ \mathrm{Inc}_{\ 2} - \ \mathrm{Inc}_{\ 9} + D_r + S_f \end{aligned} \tag{3}$$

Where C is the convolutional layer, P is the pooling layer function, Inc is the inception layer, D_r is the dropout rate, S_f is the softmax function.

- Different hidden layers have been used in the CNN model to identify wheat yellow rust disease. The identification process starts by building a feature from an input image that enables the detection of wheat rust on the wheat plant over multi-scale generated images. The output of the convolution layer is to extract features in form of a matrix. The output(O_c)comes from the convolution layer is the combination of weight(W_k) and bias(B_k) concerning the region of an image.

where the F denotes the filter/mask applied to an image, X_{ij} represents the input region of location with weight and bias respectively.

- $R_{DL} = I_s(Da/Ta) * 100$ (4)

where R_{DL} rust disease labeled image with several disease tissue in the wheat plant.

B. Dataset collection

To facilitate research into plant disease, some databases should be released openly and freely. For example determination of wheat yellow rust through conventional and wavelet spectral features [8] through 107 images of healthy and infected crops of wheat at the zodaks stage. The prediction of these diseases is very important in the agricultural industry. Wheat datasets are gathered from primary and secondary sources and expressed as follows:

- Primary sources: In primary sources, data is collected [28] through face-to-face surveys, observations, or experienced persons in real time. As a result, wheat datasets are collected from camera devices in a real-time manner, and an experienced person evaluates

TABLE I. SUMMARY TABLE OF THE RELATED WORK

# Studies	Authors and Year	Techniques	Disease	Disease Recognition	Target	Dataset Device	Location
[4]	Moshou et.al[2004]	SOM and NN(multiple perceptrons)	Rust	SOM (99%), NN (95%)	Stripe	Camera	Rothamsted Research (UK)
[5]	Mo[2010]	Backpropagation neural network	Rust	BP (89%)	Stripe	Camera	Pingliang, china
[6]	Wang and Ma[2012]	Backpropagation NN	Rust	Backpropagation NN (75%)	Stripe	Camera	Hanzhong, china
[7]	Wang et. al[2012]	Generalized regression networks (GRNN), probabilistic neural networks(PNN), Radial basis function(RBF)	Rust	NN (95%), PCA (88.33%)	Stripe, leaf	Camera	Beijing, china
[27]	Huang et. al[2012]	CNN, SVM	Blight	CNN(91.43%), SVM with vegetation index(87.65%)	Leaf	Phantom 4	Xinxiang, china
[8]	Zhang et.al[2014]	CWA and other conventional techniques	Rust	CWA(R^2(0.97)), Raw reflectance(R^2(0.96))	Stripe	Camera	Changping, china
[9]	Nie et.al[2014]	Bayesian network, BPNN, SVM	Rust	Bayesian network(82.29%), BPNN(81.25%), SVM(81.68%)	Stripe	Scanner	Gansu, china
[10]	Sarayloo et.al[2015]	RBF Neural Network, Multilayer Perceptrons Neural Networks	Rust, Spot	RBF(98.3%), MLP(88.7%)	Stripe, Spot	Camera	Iran
[11]	Xie et.al[2016]	SVM, Relevance vector machine	Rust	RVM (Recognition rate(7.4%)), SVM(Recognition rate(5.56%))	Stripe, leaf	Camera	
[19]	Pryzant et.al[2017]	CNN, RNN	Rust	Deep learning models(AUC(0.67))), Histogram buckets(AUC(0.53)))	Stripe, stem, leaf	CIMMYT	Ethiopia, South Africa
[12]	Lu et.al[2017]	CNN frameworks(VGG-FCN-VD16, VGG-FCN-S)	Rust	VGG-FCN-VD16 (Average aggregation (78.43%)), VGG-FCN-S (Average aggregation (48.86%))	Stripe, leaf	Scanner	Beijing, china
[13]	Raichaudhuri and Sharma[2017]	ANN, SVM	Rust		Stripe	Camera	South Asia, India
[14]	Xu et.al[2017]	Flood filter	Rust	Flood filter(recognition rate(98.6))	Leaf	Camera	Jiangsu, china
[20]	Zheng et.al[2018]	Random forest	Rust	Random forest(85.2%)	Stripe	Spectrometer	Langfang, china
[25]	Singh et.al[2018]	CNN Frameworks (VGG16, VGG19)	Rust	VGG16(86.53%), VGG19(83.9%)	Stripe	Imagenet	India
[18]	Picon et.al[2018]	Fully convolutional neural network	Rust	FCN(AUC(0.78))	Stripe, Leaf, Spot	Camera	Spain
[23]	Chen et.al[2018]	Support vector machine, Random Forest	Rust	SVM(91.45%), Random forest(93.80%)	Stripe, Leaf	Camera	Changee, China
[26]	Lin et.al[2019]	Matrix-based CNN, Alexnet, VGG16	Rust, Spot, Streak	MBCNN(0.942), Alexnet(0.827), VGG16(0.871)	Stripe, Leaf, spot	Camera	Shandong, china
[15]	Ozkan et.al[2019]	SVM, VGG16	Kernels	SVM(99.38%), VGG16(98.38%)	Kernel	Camera	Pingliang, china
[16]	Su et.al[2019]	CNN-LSVM	Rust	CNN-LSVM (90.32%), CNN-Softmax (71.25%) and CNN-SVM (54.37%)	Stripe, Leaf	Camera	Shandong, china
[21]	Zhang et.al[2019]	DCNN, Random forest	Rust	DCNN(0.85), Random forest(0.77)	Stripe	Camera	Langfang, china
[22]	Zhang et.al[2020]	Random forest, DCNN	Head	RF(R^2(0.89)), DCNN(R^2 (0.97))	Head	Camera	Anhui, china
[17]	Dong et.al[2020]	Differential amplification CNN	Rust, streak	DACNN(95.18%)	Stripe, leaf, streak	Camera	Shandong, china
[24]	Zhang et.al[2020]	Random forest, NN, SVM	Lodging	RF(precision(1.40%)), NN(precision(7.83%)), SVM(precision(4.84%)),	Lodging	UAS, camera	Shenzhen, china

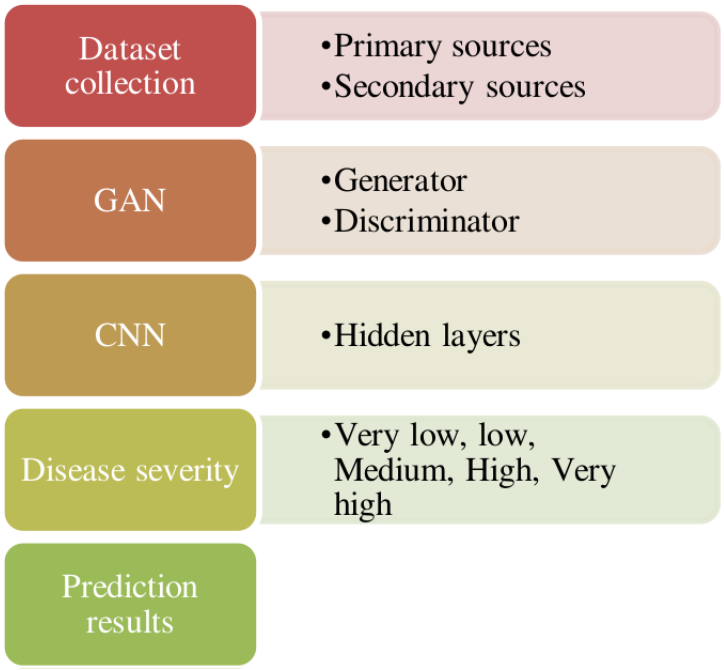

Figure 1. Overview of the proposed methodology

these data. As a result, 440 images are collected which is shown in table 2.

- Secondary sources: As a general rule, data in secondary sources is gathered from websites, web pages, and blogs [28]. For disease prediction, 360 images are collected in secondary sources which are shown in table 2.

A sampling of wheat plant images from primary and secondary sources is shown in figure 2.

C. Generative adversarial network(GAN

GAN produces synthetic images [29], and it is considered a production model.The GAN will take images from existing images dataset [29] and produces new images that are similar but different from existing or preprocessed images. The GAN is trained using a generator and discriminator. The GAN is known as a data augmentation technique in image processing. Here, we are taken as an advanced GAN variant called STARGAN for generating images. In this section, we will describe GAN-related theories. To balance the original dataset, GAN generates minority-class images with high quality.

1) Original GAN: Generally, the GAN is a two-way model. One way of the model is called a generator or production network which aims to produce new image samples from existing images. Another way of the GAN model is known as discriminator or discriminatory network and it distinguishes generated images from real images. In GAN, the generator is associated with an enemy called a discriminator. Both generator and discriminator are multilayer perceptrons. The overview of original GAN is shown in figure 3.

The description of Generator (G) and Discriminator (D) is described as:

- Generator (G): As the name of the generator describes that it generates images from real images or scratch images. It adds some noise as random input to a real image. Suppose the original image I_m and its given. During the training of an image, we are taken a sample of a latent code Y and latent code Z randomly and generate a target output T_{img}=F(Z)*Y. The generator takes an input image I_{img} and S inputs and learns to generate an output image G(I_{img}, S) through either adversarial loss or noise loss:

$$I_{adv} = EI_{im}^{x}\left[\log Dx\left(I_m\right)\right] + EI_{im},^{y,z} \left[\log\left(1 - D_z\left(G\left(I_{img}, s\right)\right)\right)\right] \quad (5)$$

Where Dx denotes the output image with domain x. The mapping F learns to provide with target style Iimg=F(Z)*Y. The G(I_{img}, S) describes the generator of an original image with domain-specific style S. The F(z) explains the mapping network and EI_{img}, X describes the style encoder of a given image with a corresponding domain. The D_Z presents the discriminator of an image.

- Discriminator (D): The discriminator takes images

Figure 2(a): Wheat yellow rust on wheat plant

Figure 2(b): Wheat yellow rust on wheat plant

Figure 2(c): Wheat stem rust on wheat plant

Figure 2(d):Wheat powdery mildew on wheat plant

Figure 2(e): Wheat healthy plant

Figure 2(f): Wheat leaf rust on wheat plant

Figure 2. Samples of wheat plant images

TABLE II. DESIGN OF WHEAT DISEASE DATASET

Wheat diseases	Primary sources	Secondary sources
Yellow rust	100	110
Leaf rust	80	70
Powdery mildew	90	60
Stem rust	60	50
Healthy plant	110	70

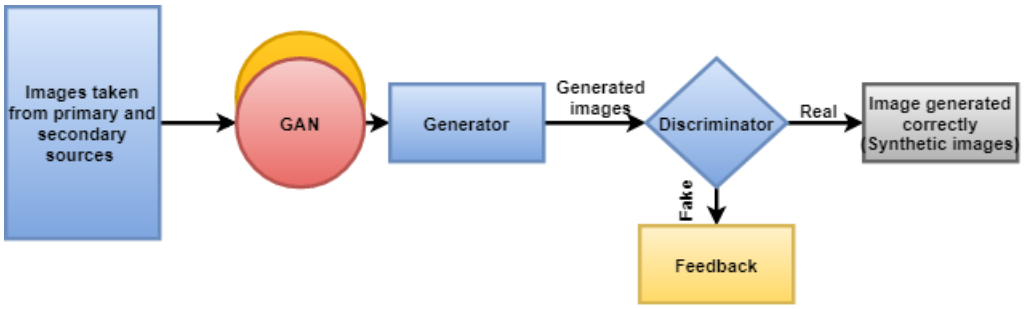

Figure 3. Proper overflow of original GAN

from the generator side as input and compares the generated image with the real image. The discriminator role is a checker. During the training of discriminator, the discriminator will check the image according to the probability distribution function. If P(d)=1 then the image is real, if P(d)=0 then the image is fake. The P denotes the probability distribution function and d denotes the data in form of images. But some images are fake during the training of the discriminator, hence data are lost. If the image is real then the equation is substituted as:

$$L_D(1) = \log(D(x)) \tag{6}$$

The loss function is denoted as L_D. If the image is fake then an equation is substituted as:

$$L_D(0) = 1 - \log(D(x)) \tag{7}$$

The maximum loss function can be calculated through the combination of Eq 6 and Eq 7 which is written as:

$$L_D = \text{Max}(\log(D(x)), 1 - \log(D(x))) \tag{8}$$

- STARGAN: Although GAN is capable of handling a pair of image domains independent of each other, it is limited in its scalability and robustness [29]. GAN's limitation is addressed by the use of StarGAN. STARGAN [30] is a novel and scalable method for performing image-to-image translations for a variety of domains. To translate the image with different colors, STARGAN has been used. With the help of STARGAN, multiple different colored images can be generated from a single image. STARGAN training has produced three types of losses, namely adversarial losses, reconstruction losses, and domain classification losses.

- Adversarial loss: To generate multiple images from a single image, the adversarial loss is denoted as:

$$L_{adv} = \text{Max}(\log(G(x)), 1 - \log(G(x))) \tag{9}$$

Equation (5) shows the adversarial loss of an image while generating the images. The L_{adv} denotes the adversarial loss and G denotes the generated image.

- Domain classification loss: The main purpose of this loss is to optimize the generated image loss corresponding to original image which is denoted as G.

$$L_{cl} = I_{img}\left[-\log D_{cl}\left(c' \mid x\right)\right] \tag{10}$$

where the L_{cl} is the classification loss, I_{img} denotes input image and D_{cl} illustrate the probability distribution over domain labels estimated through D. Before reducing the objective loss, D enroll to distinguish the real image x from its real domain c.

• Reconstruction loss: By reducing the adversarial and reconstruction loss of an image, G is trained to produce realistic and fragmented images in their proper context. However, for minimizing adversarial and domain classification loss Eq 9 and Eq 10 do not ensure that translated images retain the content of their input images while modifying only the part associated with the inclination of the input.

$$L_{rl} = I_{img}\left[x - T\left(T\left((x, c), c'\right)\right.\right. \tag{11}$$

The L_{rl} represents the reconstructed loss image, T denotes the translated image and the original domain label c'as an input that needs to reconstruct the original image x.

• Final objective: The main purpose of STARGAN is to translate the original image with minimum loss. Finally, to optimize the loss of D and G to translate the image, the equation is written as:

$$Lg = L_{adv} + L_{cl} + L_{rl} \tag{12}$$

where Lg denotes the final loss of an image.

2) *Convolutional neural networks (CNN):* CNN can get an effective presentation of an image [4], that enables us to see direct view patterns from green pixels for small to medium [12]. The design and hidden layers of CNN are depending upon the hidden layers. The main components of CNN are sparse [27] connectivity between neurons along with their shared weights and pooling. The CNN layers are described as:

- Convolution layer: The convolution layer clips input in form of images either from a built-in dataset or real-time devices. The mask/filter is applied to an image. The main functions of this layer are to preprocess the image and extract particular features from images. The output of the convolution layer is to extract features in form of a matrix. The output(O_c)comes from the convolution layer is the combination of weight(W_k) and bias(B_k) concerning the region of an image. The equation of the convolution layer is as:

$$O_c = F\left((W_k)\, X_{ij} + B_k\right) \tag{13}$$

where the F denotes the filter/mask applied to an image, X_{ij} represents the input region of location with weight and bias respectively.

- Activation function: An unsaturated output results from the convolution layer. For saturation, the activation function is used. Mostly relu, sigmoid, and TanH activation function is used for saturation. The activation function is important because it cannot saturate if a neuron activates. As long as the neuron is not activated or in a dead condition for a long time, then the activation function evaluates that neuron.

- Pooling layer: The principal function of the pooling layer is to decrease the size of the parameters used for computation. It reduces the more complicated parameter sizes when it comes from the convolution layer. The main aim of pooling layer is to reduce the pixel dimensions. There are two pooling functions namely max-pooling and average pooling used for reducing feature parameters. In max-pooling, the max parameter is taken from the array stride but in average pooling, it takes an average of all array strides.

- Overfitting and underfitting: Sometimes, training data is fit for input and does not fit for the testing dataset. So this problem occurs during data training and testing. When the training data is fit for input but does not achieves good performance during testing, and then overfitting problem is occurring. But the underfitting problem occurs when training and testing data don't fit the model. To overcome the problems of overfitting and underfitting, the dropout rate is adopted. As a result of dropout, the output of hidden neurons is set to zero with a predefined probability.

- Fully connected layer: Generally, this layer has a bias parameter. Unlike the prelayer neurons, the neurons in the end layers are fully connected, meaning they have a direct connection to the following layer neurons. The main function of the this layer is to convert the matrix data which comes either from the pooling or convolution layer and then this layer converts the matrix data into vector form for visualization purpose. CNN is a combination of hidden and fully connected layers.
- Softmax: An activation function referred to as Softmax is applied to the last layer of a CNN instead of all activation functions. The softmax function is implemented in fully connected layer. Sometimes the fully connected layer with softmax function implementation is known as dense layer.

Generally, the description of each layer in CNN is described in the above section. After the Softmax activation function extracts some probability distribution samplings which are very useful for classification purposes. The classification through CNN is described in figure 4:

D. Disease severity

In general, plant diseases are measured through intensity. For the calculation of intensity, disease severity is used. The disease severity [8] is calculated through the disease infection index. For finding the disease intensity of leaves, viruses, and bacterial diseases the disease incidence is calculated. But for calculating the intensity of rust diseases disease severity is used.

The severity of the disease is the percentage of appropriate tissues covered by the disease. Disease severity is more appropriate for rust-based diseases. An experienced investigator will fix the disease severity index labels through visual inspection. The investigator will fix the severity labels according to wheat image samples. The Disease intensity was calculated from the range of 0-100%. The severity levels were evaluated by the investigator along with the labeling which has been shown in table 3. The disease severity is calculated on the behalf of many rust-based tissues on the wheat plant. Once, the rust-based tissues on the wheat plant have been determined, the severity has been calculated. The severity ranges between 0-20percent and is considered a healthy plant.

4. Experimental results and discussions

A. Experimental steup

All the experiments are performed on a Dell desktop with having Win 10 operating system Intel (R)Core(TM) i5-6300HQ CPU @2.30 GHz, 16.00 GB RAM, and NVIDIA Geforce GTX 960 M GPU. For implementation, we use python 3.6.1 with TensorFlow and the scikit learn library for practical simulations.

B. Hyperparametres tuning

A 124-neuron two-layer neural network is used to generate a network by the generator and discriminator. The data generated and then challenged were placed in the standard range after the model training process was completed. The hyperparameters which are used for implementing STARGAN and CNN are shown in table 4(a),(b).

C. Synthsized images generated through STARGAN

The main objective of GAN is to generate synthesized images from an original image. The synthesized image is made according to style reconstruction and color diversification. The wheat-augmented images generated by GAN are shown in figure 5:

The generated dataset with the different numbers of wheat diseases in a balanced way is shown in table 5.

D. Architecture details of proposed method

After data augmentation through StarGAN, an entire of 4000 wheat plant images are generated. Among the generated images, a number of 2800, 1200 augmented images have been used for training and testing purposes in CNN model. The details of CNN network architecture along with different layers have been shown in table 4.

Table 6 describes the mask with size applied to the input image and output corresponding to that image respectively. The prediction of wheat yellow rust starts by resizing the image in 436*436 pixels and dividing the images into two grids 29*29 and 58*58 which are responsible for performing the prediction of wheat yellow rust at two different scales. CNN will apply to the severity levels of data.

E. Model training and testing

In the classification stage, the CNN2D model consists of 3 convolution layers with kernel sizes 1*1, 2*1, and 3*2 correspondingly. But in the pooling layer, the max pooling function with size 2*2 is used. During training, the number of epochs is compared for improving accuracy. The kernel size of the max pooling layer in CNN2D is set to be 2*2.

- Measuring STARGAN accuracy through training loss: Figure 6(a) presents the discriminator loss of real and fake images as 0.5 and generally generator loss lies between 0.0 to 1.5. The loss of fake and real images with the discriminator is compared with several epochs. Figure 6(b) shows the discriminator

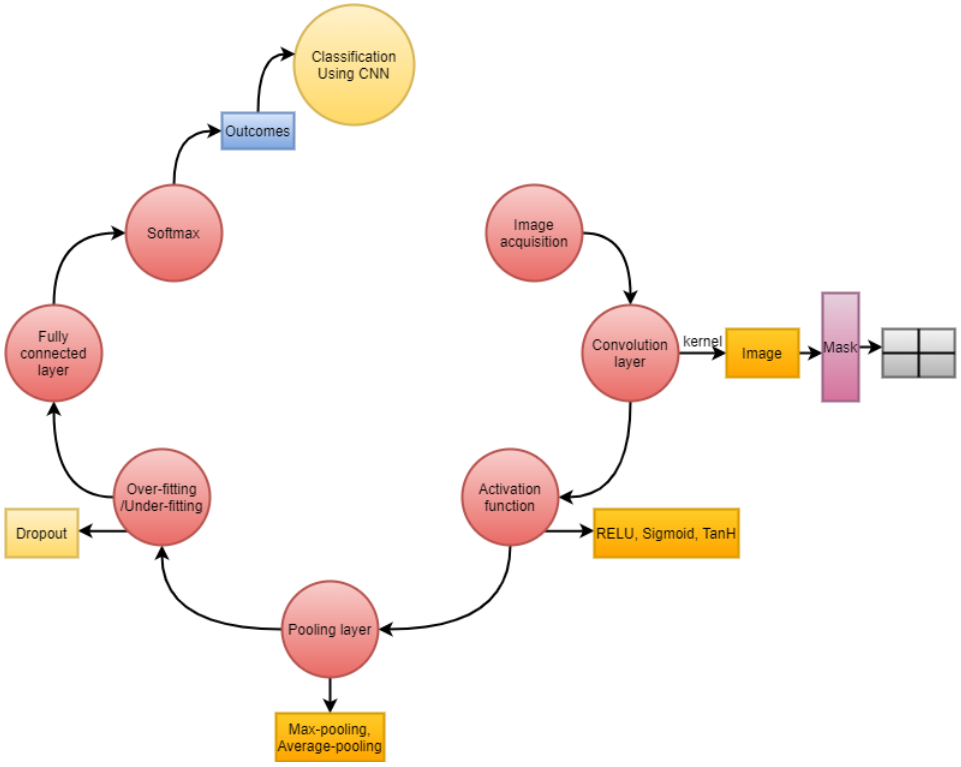

Figure 4. Overview of CNN

TABLE III. DISEASE SEVERITY LEVELS

Range (%)	**Labels**
0-20	Very low
20-40	Low
40-60	Medium
60-80	High
80-100	Very high

TABLE IV(A). HYPERPARAMETERS USED FOR STARGAN IMPLEMENTATION

STARGAN Hyperparameters			
Activation function	Parameters(Millions)	Optimizer	Input noise(Generator)
Relu	53.2	Adam	60
CNN Hyperparameters			

TABLE IV(B). HYPERPARAMETERS USED FOR CNN IMPLEMENTATION

Activation function	Optimizer	Batch size	Number of epochs	Pooling layer	Number of neurons
Relu	Adam	16,32,64	100	Max Pooling	100

TABLE V. GENERATED DATASET WITH WHEAT DISEASES

Wheat diseases	**Collected images**	**Augumented images (Ratio 1:5) for every disease images**
Yellow rust	210	1050
Leaf rust	150	750
Powdery mildew	150	750
Stem rust	110	550
Healthy plant	180	900

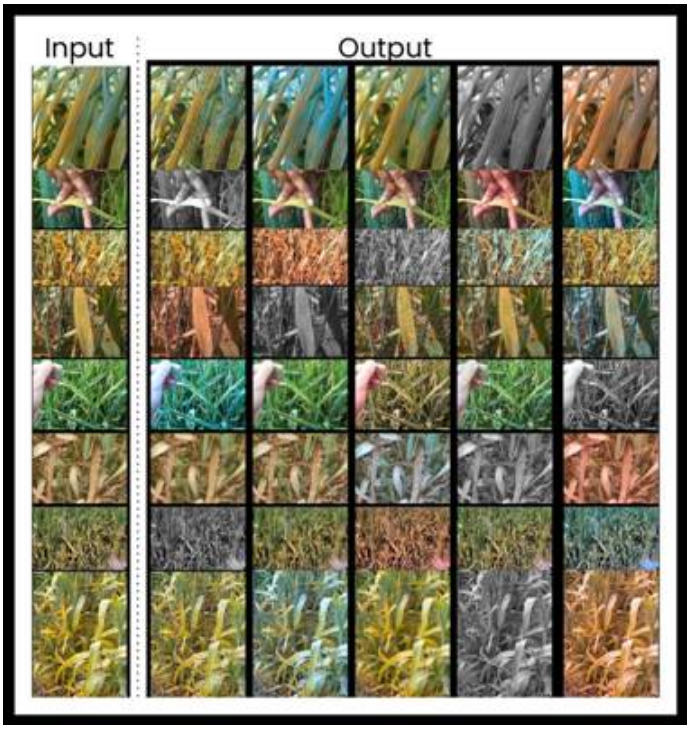

Figure 5. Synthsized images generated through STARGAN

TABLE VI. DETAILED CNN NETWORK ARCHITECTURE

#	Layers(CNN)	Mask	Size	Input	Output
1.	Convolution	16	3*3/1	464*436*3	464*464*16
2.	Max pooling		2*2/2	464*436*16	232*232*16
3.	Convolution	32	3*3/1	232*232*16	232*232*32
4.	Max pooling		2*2/2	116*116*32	116*116*32
5.	Convolution	64	3*3/1	116*116*32	116*116*64
6.	Max pooling		2*2/2	116*116*64	58*58*64
7.	Convolution	128	3*3/1	58*58*64	58*58*128
8.	Max pooling		2*2/2	58*58*128	29*29*128
9.	Convolution	256	3*3/1	29*29*128	29*29*256
10.	Max pooling		2*2/2	29*29*256	29*29*256

accuracy on real(blue) and fake(red) during training with different severity levels.

- CNN training and testing: In training, 100 neurons have been used in the fully connected layer. For training and testing, we have used different batch sizes (16, 32, 64) with batch size 100 compared to measuring the accuracy of the model. The training and validation loss of CNN with different severity is shown in figure 7(a). The training and testing accuracy of CNN in real and augmented images is shown in figure 7(b).

F. Wheat rust identification results

For data augmentation, GAN is used. But for identification whether the wheat plant is infected by yellow rust or not.Figure 8(a) shows the example of wheat yellow rust sampling corresponding to the pattern or yellow rust diseased area on the wheat plant.The mapping of wheat yellow rust on the wheat plant is achieved through CNN modelresults show that wheat yellow rust at medium-level severity is checked. After testing, the CNN approach achieves high classification accuracy (95.6%) using GAN-augmented images. Figure 8(b) shows the localization of wheat yellow rust on the wheat plant.

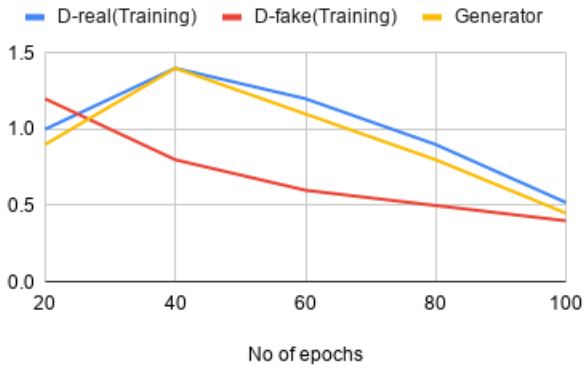

Figure 6(a). Discriminator loss of real and fake images(StarGAN)

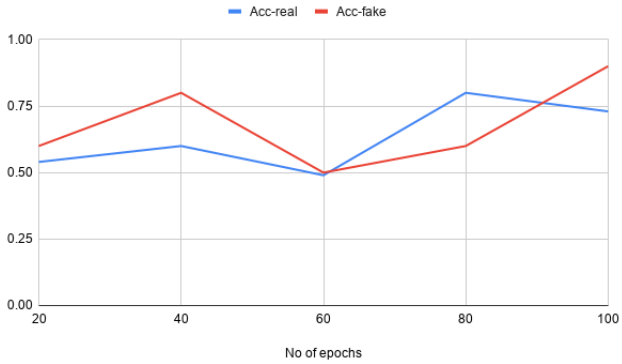

Figure 6(b). Discriminator accuracy of real and fake images

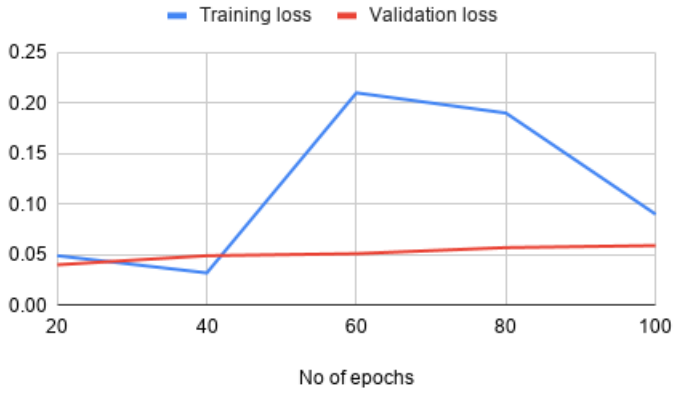

Figure 7(a). Training and validation loss of CNN during wheat-augmented images

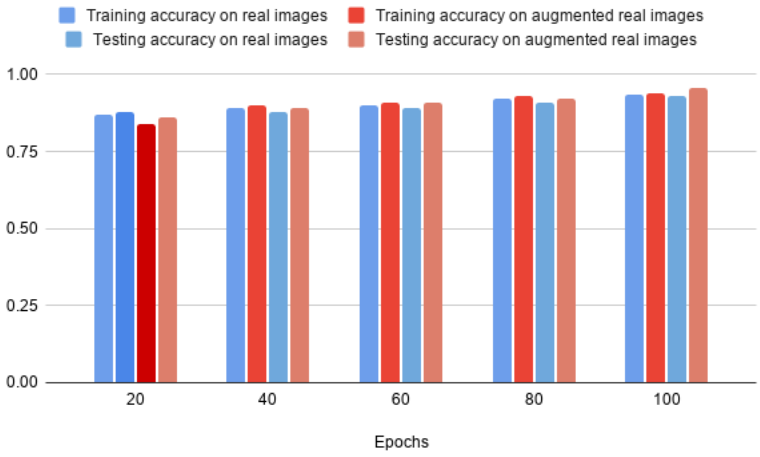

Figure 7(b). Training and testing accuracy of CNN over augmented and real images

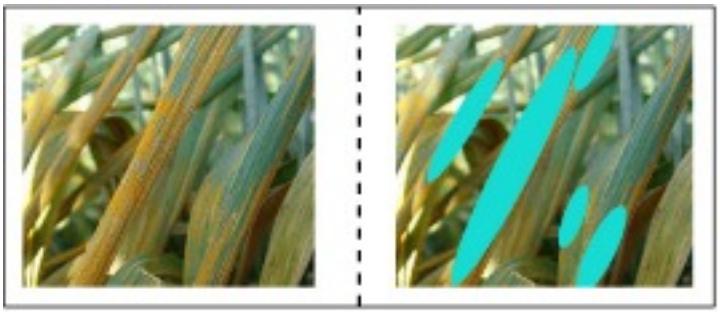

Figure 8(a). Example of Wheat yellow rust corresponding to the mapping of yellow rust on wheat plant

Figure 8(b). localization of wheat yellow rust through the proposed approach

5. Performance analysis of proposed approach

Generally, GAN+CNN is a proposed technique for wheat disease prediction specifically. But the proposed hybrid technique is general and it should be suitable for other crops or vegetables, such as maize, tomatoes, peppers, etc. Since many vegetable/ plant disease dataset is not available. For increasing data augmentable, GAN is used. The GAN-augmented images are preprocessed faster to predict/classify disease easily. The CNN will train and be tested according to wheat yellow rust severity levels. Although, CNN overcomes the overfitting/underfitting problems when increasing the dataset through augmented images. Therefore the proposed technique should be modified for better accuracy. When our system needs to be expanded into other new crop diseases, all we have to do is install the corresponding channels in the deep architecture and fix it based on new class information for additional diseases. In the future, we will focus on building a strong and dynamic framework based on the current system to match the mixed conditions of many different diseases or plants, which are the most difficult challenges in diagnosing plant/crop diseases.

A small number of researchers have been purposed various techniques for wheat yellow rust identification. Therefore, for better classification of wheat rust our proposed technique is compared with previous techniques which are shown in table 7:

TABLE VII. Performance Comparison between Our Technique and State Of Art Techniques

Referenced study	Method	Dataset	Accuracy	Disease classification	Classified classes
[4]	SOM and NN(multiple perceptrons)	5137	SOM (99%), NN (95%)	Yellow rust	1
[5]	Backpropagation neural network	1025	BP (89%)	Yellow rust	1
[18]	Fully convolutional network	8178	(AUC(0.78))	Yellow rust, Leaf rust, Tan spot	3
[19]	Convolutional and long short-term memory neural networks	8554	LSTM(AUC(0.67))	Yellow rust, stem rust, leaf rust	3
[12]	CNN frameworks(VGG-FCN-VD16, VGG-FCN-S)	9230	VGG-FCN-VD16 (Average aggregation (78.43%)), VGG-FCN-S (Average aggregation (48.86%))	Yellow rust, leaf rust	2
[16]	CNN-LSVM	6028	CNN-LSVM (90.32%), CNN-Softmax (71.25%) and CNN-SVM (54.37%)	Yellow rust, leaf rust	2
[17]	Differential amplification CNN	8326	DACNN(95.18%)	Yellow rust, leaf rust, streak	3
[21]	DCNN, Random forest	10,000	DCNN(0.85), Random forest(0.77)	Yellow rust	1
[25]	CNN Frameworks (VGG16, VGG19)	634	VGG16 (86.53%), VGG19 (83.9%)	Yellow rust	1
[26]	Matrix-based CNN, Alexnet, VGG16	16,652	MBCNN(0.942), Alexnet(0.827), VGG16(0.871)	Yellow rust, Leaf rust, Tan spot	3
Our Proposed technique(GAN+CNN)	GAN+CNN	800	GAN+CNN (95.6%)	Yellow rust	1

6. Conclusion and Future Work

Identification of wheat yellow rust is a very challenging process, and it takes a lot of time and effort by an experienced evaluator. From observation of table 1, it shows that most wheat rust diseases are identified in the china area. In this paper, a computer vision generator classification model is present for wheat yellow rust disease prediction model which aims to deal with in-field wheat images without any technical preprocessing. We utilize two different deep learning models to perform wheat yellow rust disease prediction on the newly collected primary and secondary sources dataset.

After data generation, CNN achieves high training and testing accuracy of real images as compared to training and testing accuracy of fake images.

During experimentation, our proposed approach achieves 95.6% classification accuracy in the medium severity level for wheat yellow rust identification. Only two of the studies used hybrid approaches for wheat yellow rust identification.

Therefore our proposed model is suitable for increasing dataset size using GAN and achieves high classification accuracy for wheat yellow rust disease prediction in real time manner. Additionally, the proposed GAN-CNN model could be used as a mobile application for diagnosing agricultural diseases. Evaluation of proposed model in future directions for wheat diseases identification: The generated data is very helpful for the prediction of other wheat rust diseases.

Figure 9 shows that the wheat yellow rust model is helpful for the prediction of other types of wheat rust diseases with disease severity in the future.

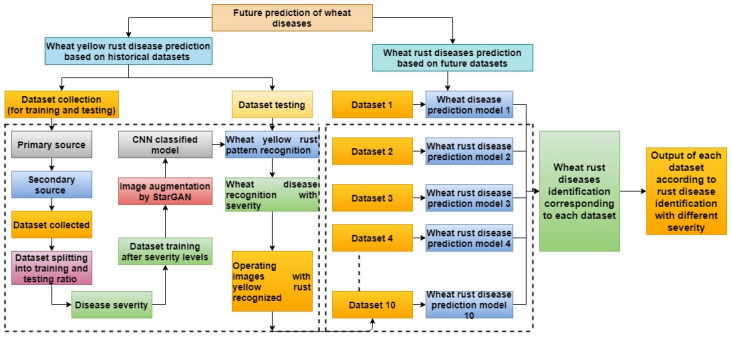

Figure 9. Wheat yellow rust disease prediction model for the future era

References

[1] "indian Wheat Rust Pathogen, *Indian Council of Agricultural Research*, pp. 12–12, 2020. [Online]. Available: https://icar.gov.in/node/4531

[2] *Wheat blast has made the intercontinental jump to Africa*, pp. 12–12, 2020. [Online]. Available: https://wheat.org/tag/wheat-blast/

[3] S. C. Bhardwaj, G. P. Singh, O. P. Gangwar, P. Prasad, and S. Kumar, "Status of wheat rust research and progress in rust management-indian context," *Agronomy*, vol. 9, no. 12, pp. 1–14, 2019.

[4] D. Moshou, C. Bravo, J. West, S. Wahlen, A. Mccartney, and H. Ramon, "Automatic detection of 'yellow rust' in wheat using reflectance measurements and neural networks," *Comput. Electron. Agric*, vol. 44, no. 3, pp. 173–188, 2004.

[5] L. Mo, "Prediction of Wheat Stripe Rust using Neural Network," *IEEE International Conference on Intelligent Computing and Intelligent Systems*, pp. 475–479, 2010.

[6] H. Wang and Z. Ma, "Prediction of Wheat Stripe Rust Based on Neural Networks," *International Conference on Computer and Computing Technologies in Agriculture*, pp. 504–515, 2012.

[7] H. Wang, G. Li, Z. Ma, and X. Li, "Image recognition of plant diseases based on principal component analysis and neural networks," *IEEE 8th International Conference on Natural Computation*, pp. 246–251, 2012.

[8] J. Zhang, L. Yuan, R. Pu, R. W. Loraamm, G. Yang, and J. Wang, "Comparison between wavelet spectral features and conventional spectral features in detecting yellow rust for winter wheat," *Comput. Electron. Agric*, vol. 100, pp. 79–87, 2014.

[9] C. Nie, L. Yuan, X. Yang, and L. Wei, "Comparison of Methods for Forecasting Yellow Rust in Winter Wheat at Regional Scale," *International Conference on Computer and Computing Technologies in Agriculture*, pp. 444–451, 2014.

[10] Z. Sarayloo and D. Asemani, "Designing a classifier for automatic detection of fungal diseases in wheat plant by pattern recognition techniques," *IEEE 23rd Iranian Conference on Electrical Engineering*, pp. 1193–1197, 2015.

[11] X. Xie, X. Zhang, B. He, D. Liang, D. Zhang, and L. Huang, "A system for diagnosis of wheat leaf diseases based on Android smartphone," *International Society for Optics and Photonics*, vol. 10155, pp. 1 015 526–1 015 535, 2016.

[12] J. Lu, J. Hu, G. Zhao, F. Mei, and C. Zhang, "An in-field automatic wheat disease diagnosis system," *Comput. Electron. Agric*, vol. 142, pp. 369–379, 2017.

[13] R. Raichaudhuri and R. Sharma, "On Analysis of Wheat Leaf Infection by Using Image Processing," *International Conference on Data Engineering and Communication Technology*, pp. 569–577, 2017.

[14] R. Z. Xu, G. Peifeng, Y. Wu, H. Guo, and Yang, "Automatic wheat leaf rust detection and grading diagnosis via embedded image processing system," *Procedia Comput. Sci*, vol. 107, pp. 836–841, 2017.

[15] K. Özkan, "Identification of wheat kernels by fusion of RGB , SWIR , and VNIR samples," *J. Sci. Food Agric*, vol. 99, no. 11, pp. 4977–4984, 2019.

[16] T. Su, S. Min, A. Shi, Z. Cao, and M. Dong, "A CNN-LSVM model for imbalanced images identification of wheat leaf," *Neural Netw. World*, vol. 29, no. 5, pp. 345–361, 2019.

[17] M. Dong, S. Mu, A. Shi, W. Mu, and W. Sun, "Novel method for identifying wheat leaf disease images based on differential amplification convolutional neural network,"," *Int. J. Agric. Biol. Eng*, vol. 13, no. 4, pp. 205–210, 2020.

[18] A. Picon, A. Alvarez-Gila, M. Seitz, A. Ortiz-Barredo, J. Echazarra, and A. Johannes, "Deep convolutional neural networks for mobile capture device-based crop disease classification in the wild," *Comput. Electron. Agric*, vol. 161, pp. 280–290, 2018.

[19] R. Pryzant, S. Ermon, and D. Lobell, "Monitoring Ethiopian Wheat Fungus with Satellite Imagery and Deep Feature Learning," *IEEE Computer Society Conference on Computer Vision and Pattern Recognition Workshops*, pp. 1524–1532, 2017.

[20] L. L. Zheng, W. Qiong, X. Huang, Y. Cui, and Shi, "New spectral index for detecting wheat yellow rust using Sentinel-2 multispectral imagery," *Sensors*, vol. 18, no. 3, pp. 1–19, 2018.

[21] X. Zhang, "A deep learning-based approach for automated yellow rust disease detection from high-resolution hyperspectral UAV images," *Remote Sens*, vol. 11, no. 13, pp. 1–16, 2019.

[22] D. Y. Zhang, "Integrating spectral and image data to detect Fusarium head blight of wheat," *Comput. Electron. Agric*, vol. 175, pp. 105 588–105 600, 2020.

[23] D. Chen, Y. Shi, W. Huang, J. Zhang, and K. Wu, "Mapping wheat rust based on high spatial resolution satellite imagery," *Comput. Electron. Agric*, vol. 152, pp. 109–116, 2018.

[24] Z. Zhang, P. Flores, C. Igathinathane, D. L. Naik, R. Kiran, and J. K. Ransom, "Wheat lodging detection from UAS imagery using machine learning algorithms," *Remote Sens*, vol. 12, no. 11, 2020.

[25] R. Singh, R. Rana, and S. K. Singh, "Performance Evaluation of VGG models in Detection of Wheat Rust," *Asian J. Comput. Sci. Technol*, vol. 7, no. 3, pp. 76–81, 2018.

[26] Z. Lin, G. S. Member, S. Mu, and F. Huang, "A Unified Matrix-based Convolutional Neural Network for Fine-Grained Image Classification of Wheat Leaf Diseases," *IEEE Access*, vol. 7, pp. 11 570–11 590, 2019.

[27] H. Huang, J. Deng, Y. Lan, A. Yang, and L. Zhang, "Detection of Helminthosporium Leaf Blotch Disease Based on UAV Imagery," *Appl. Sci*, vol. 9, no. 3, pp. 558–570, 2012.

[28] *Primary and Secondary Source Data*, pp. 18–18, 2020. [Online]. Available: https://keydifferences.com/difference-between-primary-and-secondary-data.html

[29] J. Rocca, *Understanding Generative Adversarial Networks," Towards Data Science*, pp. 18–18, 2019. [Online]. Available: https://towardsdatascience.com/understanding-generative-adversarial-networks-gans-cd6e4651a29

[30] J. C. Choi, M. Choi, M. Kim, J.-W. Ha, and S. Kim, "StarGAN: Unified Generative Adversarial Networks for Multi-domain Image-to-Image Translation," *Conference on Computer Vision and Pattern Recognition*, pp. 8789–8797, 2018.

Deepak Kumar is received his Master of Engineering degree in Computer science and Engineering from Chitkara University, Punjab. He has published more than 10 research papers in reputed international journals and conferences. His research interests include Data Analytics, Machine Learning, Deep learning and Image Processing.

Dr. Vinay Kukreja completed his Master's Degree from Punjabi University and his Ph.D. in Computer Science & Engineering from Chitkara University. He has a total teaching experience of more than 16 years. He is presently working as a Professor at Chitkara University, Punjab, India. His areas of research interest mainly include machine learning, deep learning, agile software development, decision-making approaches, and structural equation modeling.